AADE-25-NTCE-053

High-frequency Embedded Drilling Dynamics Data is Helping to Reduce Permian Basin Drilling Costs

Steve Jones, Junichi Sugiura, and Zach Ference, Sanvean Technologies

Abstract

Permian drillers are pushing downhole equipment to the limit in search of maximum rate of penetration (ROP) and improved cycle times. The time and cost of tripping for dull/damaged drill bits and mud motor failures is a major focus for all operators. High-frequency embedded drilling dynamics sensors are being selectively used with the primary purpose of understanding damaging downhole dynamics.

Placement of these sensors at the bit and above the motor power section delivers valuable data to identify drilling issues and make decisions to produce fast wells with repeatable results. High-magnitude drilling dynamics are always going to be present when drilling to the limit. The art of the game is to understand how to manage these dynamics for maximum ROP and equipment life.

The data gathered showed that damaging dynamics were driven by formation, bottom-hole assembly (BHA) design, self-induced from operating parameters and operational techniques, or a combination of some or all. Once the primary forces were identified, the damages were reduced, and well delivery consistency was improved.

This paper will provide a compilation of the latest drilling dynamics discoveries from embedded high-frequency sensors that were utilized on conventional steerable motor and rotary-steerable (RS) drilling assemblies.

Introduction

Embedded high-frequency drilling dynamics data recorders are now a standard tool for the Drilling Engineer. Although they are not run on every well, they are strategically placed on certain wells to “spot check” drilling dynamics and make incremental changes for performance gains.

Experts in the drilling domain have changed their opinion on drilling dynamics measurements, placement and method of data transfer (memory or real-time). It has long been the industry standard for drilling dynamics measurements to be transmitted in real time from an measurement-while-drilling (MWD) tool (Close et al. 1988; Zannoni et al. 1993). The advent of embedded high-frequency drilling dynamics data recorders, that can be placed anywhere in the BHA, have uncovered a different approach to gather data that cannot be seen from traditional MWD measurement and placement (Jones et al. 2017; Sugiura & Jones 2019; Sugiura & Jones 2020; Sugiura & Jones 2021).

Embedded high-frequency drilling dynamics sensors are data recorders and not real-time devices. The main reason for this is threefold:

1. **Placement** – The device can be placed in the drill bit or anywhere in the BHA to gather the high-frequency dynamics at the points of interest (Jones et al. 2017).
2. **Data transfer** – High-frequency data (800Hz) cannot be transmitted by short-hop or mud pulse MWD tools because of their limited data rates. Data transfer for high-frequency sensors is only possible through high-speed memory download (i.e. post-run download and processing).
3. **Reliability and cost** – Since these devices are typically placed at the drill bit, the dynamics levels can be severe, so increased reliability is obtained through less complexity, hence memory devices are best suited for this application.

The methodology of dealing with high-frequency memory-based drilling dynamics data, rather than real-time MWD drilling dynamics data, is different. Typically, MWD dynamics measurements are transmitted in real time, and surface parameters are optimized to control the dynamics to an acceptable level. If the MWD tool is placed above the motor, then the dynamics that are seen by the MWD are related to drillstring dynamics (and not bit dynamics). Drilling parameter changes to optimize drillstring dynamics may have minimal effect on drill-bit dynamics.

This is where embedded drilling dynamics data recorders change the reality of drilling dynamics measurements. Placement of an embedded high-frequency drilling dynamics data recorder at the bit, and correlating this with MWD dynamics data, will clearly show the difference between the two measurement placements. Once this is understood, then the benefit of embedded high-frequency drilling dynamics data recorders will become apparent.

Embedded Sensor Construction, Measurements and Placement

The embedded high-frequency drilling dynamics sensors are constructed in two different form factors to aid optimal placement in the drill bit and bottom-hole assembly (BHA).

Fig. 1 shows the construction of the sensors.

Fig. 1—Embedded sensor construction.

Shock and gyro sampling rates can be adjusted to suit the application and placement of the sensor. A high temperature option for the sensor is now available. **Fig. 2** shows the specification of the sensors.

Description	High-frequency Data Recorder
Placement	Drill Bit Shank, BHA and Drill String
Logging Trigger	RPM or RPM Delay
3-Axis Shock	-200G to +200G (+/- 100mG)
Shock Sample Rate	800 to 1600Hz
Shock Record	Continuous
Gyro RPM	+/- 330 RPM, up to +/-1000 RPM
Gyro Sample Rate	100 to 1000Hz
Gyro Record	Continuous
Temperature	150C (302F) 175C (347F) – Option Available
Pressure Rating	15,000 PSI
Recording Life	150 Hours at 800Hz 100 Hours at 1600Hz

Fig. 2—Embedded sensor specification.

The embedded sensors have been constructed to allow easy placement anywhere in the drill bit and BHA components. The design allows for outer-diameter (OD) and centerline mounting options, giving flexibility to select optimal placement for the environmental conditions of the project. **Fig. 3** shows the embedded sensor placement options (and accelerometer axis convention).

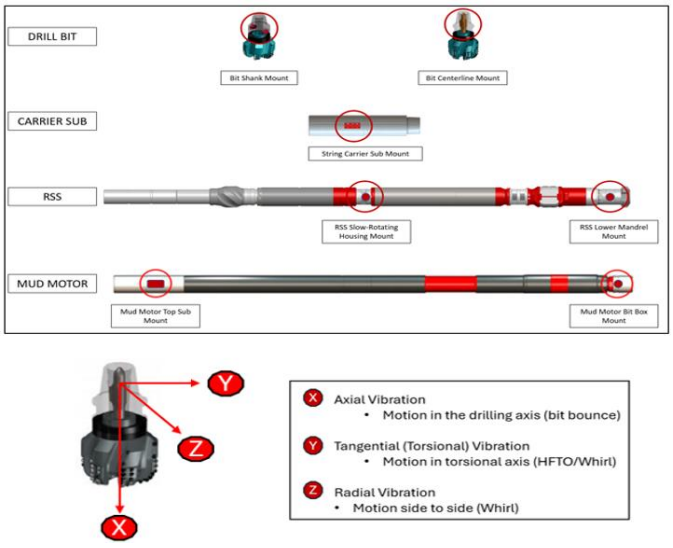

Fig. 3—Embedded sensor placement and accelerometer axis convention.

Sensor placement can be defined by two components:

1. Placement with reference to axial length from drill bit (i.e. measured axial length to each sensor from bit).
2. Placement with reference to collar radius or radial offset distance (i.e. OD mount or centerline mount).

Understanding these sensor placement components is necessary for accurate interpretation and analysis of the data gathered from each sensor.

The Importance of Drilling Dynamics Measurement Placement

When a mud motor is used in the BHA, certain high-frequency and low-frequency dynamic coupling will become apparent (Sugiura and Jones 2019; Sugiura and Jones 2020). Understanding this coupling will help diagnose the primary drilling dynamics dysfunction from the bit and BHA.

Fig. 4 shows the difference in 3-axis shock response (from the accelerometers) based on the sensor placement. Utilizing OD-mount embedded sensors in the drill bit and mud-motor top sub, the shocks at the bit typically read higher than shocks at the top sub. This is because of placement relative to the power section.

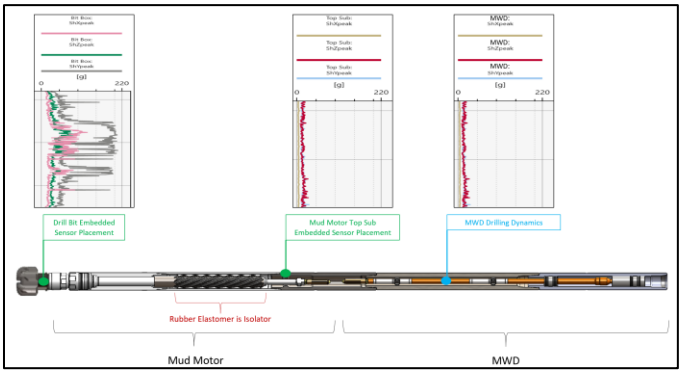

Fig. 4—Shock response difference based on sensor placement.

The sensor placed at the bit will measure the interaction of PDC cutters with the rock on the output of the power section. This is a high-frequency dynamic component that will not pass up through the motor power-section elastomer (isolator) and cannot be seen at the motor top sub embedded sensor or MWD dynamics sensors.

The sensor placed in the motor top sub (above the motor power section) will measure the string input shock to the motor, and the reaction shock of the motor power section (reactive torque, while slide drilling or back-drive, while rotary drilling).

The response of the sensor placed in the MWD will depend on the design of the MWD tool. A basic MWD string loaded into a rental collar will have dynamics sensors that are mounted on centerline. Because the mounting of the MWD inside the collar is not ideal for shock measurements, the transmissibility of the dynamic measurement may be high.

Care should be taken when interpreting these different placements and measurements. Distance from bit, placement relative to motor power section, OD or centerline mount and MWD mount all affect the shock dynamic measurements.

Fig. 5 shows the difference in torsional response (from the gyro) based on sensor placement. Utilizing OD or centerline mounted embedded sensors in the drill bit and mud motor top sub (or carrier sub), the gyro measurements will show a different response. This is because of placement relative to the power section.

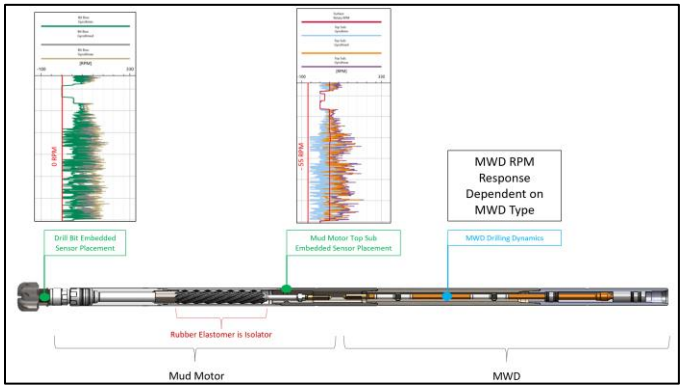

Fig. 5—Torsional response (RPM) difference based on sensor placement.

The sensor placed at the bit will measure the torsional interaction of PDC cutters with the rock on the output of the power section. This is a high-frequency dynamic component that will not pass up through the motor power section elastomer (isolator) and cannot be seen at the motor top sub embedded sensor or MWD dynamics sensors (Sugiura and Jones 2020).

The sensor placed in the motor top sub (above the motor power section) will measure the string torsional input to the motor, and the torsional reaction of the motor power section (reactive torque, while slide drilling or back-drive, while rotary drilling).

The response of the sensor placed in the MWD will depend on the design of the MWD tool. A basic MWD string may not contain gyro measurements. The RPM measurement will be derived from accelerometer and/or magnetometer measurements and may not be capable of providing negative RPM, especially the real-time transmitted MWD rotation speed.

Once again, care should be taken when interpreting these different placements for RPM measurements. Placement relative to motor power section and MWD RPM measurements (gyro or derived from another source), all affect the torsional dynamic measurements.

Drilling Dynamics Discoveries with High-frequency Embedded Sensors

Placement of multiple embedded high-frequency drilling dynamics sensors at specific points of interest in the bit and BHA, can deliver a suite of data that can aid in understanding the primary driving mechanism behind dynamics that can cause premature bit wear/damage, power section degradation and /or chunking and tool failures.

The main dynamic influences for drill-bit/BHA performance and longevity are:

1. Bit type
2. Motor power section type
3. Motor configuration (bend angle and stabilization)
4. RSS type (fully rotating or slow-rotating steering mechanism)
5. BHA design (collars, heavy-weight drill-pipes and drill-pipes)
6. BHA stabilization (slick or stabilized, and stabilizer type)
7. Formation type (e.g. interfacial severity) (Pastusek et al. 2018; Dupriest et al. 2020)
8. Mud type
9. On-bottom rig control (auto-driller limits, drilling-advisory-system limits) (Pastusek et al. 2016; Adam 2018)
10. Transitional rig control (manual or automated)

All the above items need to be considered when analyzing drilling dynamics. The one item that we have no control over is formation. The BHA may be used to drill through multiple formations in an intermediate section of the wellbore. Understanding the formations that drive damaging dynamics is the key to drilling efficiently. Fast pace with high dynamics in forgiving formations versus controlled pace through damaging formations is the art of accurate road mapping.

High-frequency Torsional Oscillations (HFTO)

High-frequency torsional oscillation dynamics have gained a lot of interest in recent years, particularly with motor-assist RSS BHAs (Lines et al. 2013; Oueslati et al. 2013; Jain et al 2014; Sugiura & Jones 2019; Sugiura & Jones 2020). This is because of the damage that can be induced on the equipment below the mud motor, particularly RSS and MWD. HFTO is thought to originate from very high-frequency shocks generated by the interaction between the Polycrystalline Diamond Compact (PDC) cutters and formation, which resonates with the lower BHA structure (Pastusek et al. 2007; Oueslati et al. 2013; Jain et al 2014). The HFTO energy remains trapped below the mud motor because the HFTO energy resonates to the structure below the motor and the motor power-section elastomer acts as a dampener.

The trapped HFTO energy can cause rapid torsional fatigue on the OD of BHA mechanical components (e.g. RSS bias and control unit) and electrical components (Watson et al. 2022). The cost of this fatigue damage can be very high. **Fig. 6** shows an example of high HFTO and how it is seen in the BHA.

The highest HFTO levels are seen at the drill bit (180G tangential [or approximately 23,662 rad/s2] sustained and 110Hz). Below the motor, at the bearing mandrel, the HFTO G-level is slightly lower (110G tangential [or approximately 14,460 rad/s2] sustained) because of the distance from the bit. The frequency remains the same at 110Hz.

Above the motor, no HFTO can be seen. The tangential and radial shocks are low at less than 30G. This is because the motor rubber elastomer acts as an isolator and the HFTO generated below the motor cannot pass to the stator/top sub of the motor.

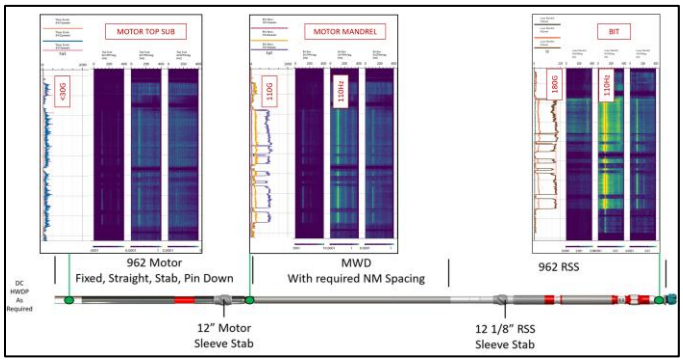

Fig. 6—HFTO on motor-assist RSS BHA.

The addition of an HFTO suppression tool below the motor has become commonplace to reduce RSS damage. **Fig. 7** shows an example with an HFTO suppression tool in the BHA.

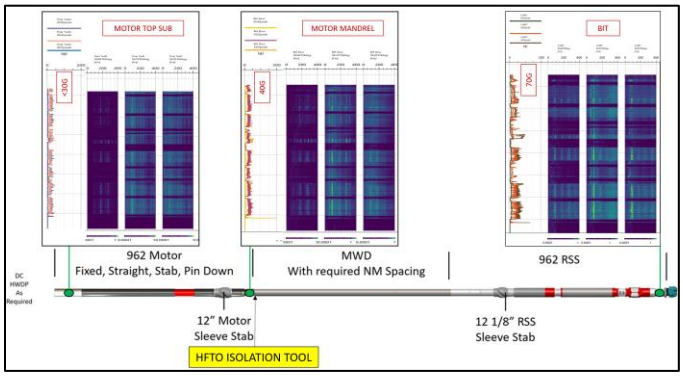

Fig. 7—HFTO reduction on motor-assist RSS BHA.

The HFTO magnitude at the bit has been reduced to 70G [or approximately 9,202 rad/s2] at the drill bit, compared to 180G [or approximately 23,662 rad/s2] previously. Below the motor, at the bearing mandrel, the HFTO G-level is 40G [or approximately 5,258 rad/s2], compared to 110G [or approximately 14,460 rad/s2] previously. Above the motor, the tangential and radial shocks are less than 30G.

This reduction in sustained tangential G-levels reduces the torsional fatigue on RSS components and improves reliability.

Embedded high-frequency drilling dynamics sensors are very useful in understanding the effectiveness of an HFTO mitigation tool. It is common in North America land for operators to measure the effectiveness of the various HFTO tools available on the market.

As mentioned, placement of the sensor relative to BHA position from bit is important. However, sensor placement with reference to the centerline of BHA is also important when analyzing HFTO data. Normally, tangential accelerations from high-frequency accelerometers are used to measure HFTO magnitude on outboard mounted sensors and high-frequency gyro measurements are used to measure HFTO magnitude on centerline mounted sensors. **Fig. 8** shows a comparison of measurements from drill bit shank (outboard) and centerline mount sensors.

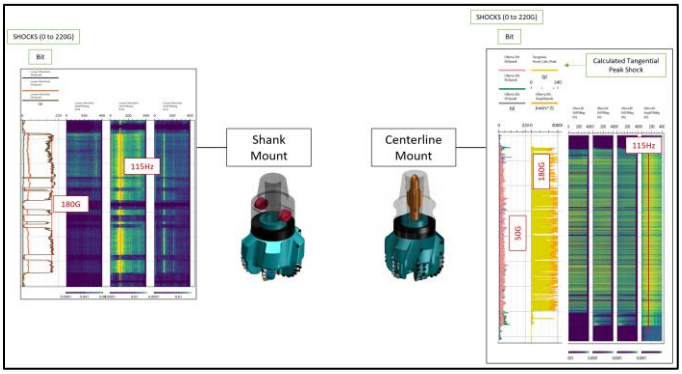

Fig. 8—Comparison of drill bit shank and centerline mount placement.

Mud Motor Back Drive (MMBD)

Stick-slip is a well-known type of torsional dynamics in which a drill bit and/or drillstring change their rotation speed periodically, alternating "stick" and "slip" phases (Halsey 1986; Kyllingstad & Halsey 1987; Brett 1992). The stick-slip phenomena have been researched for many years; however, mud motor back-drive (MMBD) dynamics has only been relatively recently recognized and studied. In motor back-drive dynamics, the bit comes to a complete stop (bit stall) and the motor drives the drillstring backward (Sugiura & Jones 2021; Sugiura et al. 2022). MMBD dynamics are common on conventional steerable motor BHAs as well as motor-assist RSS BHAs (Jones et al. 2023). The sequence of events of mud motor back drive are as follows –

1. Rotary drilling ahead.
2. Drill bit stalls (bit "stick" phase).
3. Mud motor power section does not stall, it back-drives torque/RPM up the drill string.
4. When the surface torque/RPM meets the back-drive torque/RPM, there is a sudden release of torsional energy.
5. This causes the bit and BHA to suddenly accelerate up to high RPM (bit "slip" phase).
6. The drill bit stalls again (bit "stick" phase).
7. The cycle repeats.
8. A torsional neutral point moves up and down the drill string as the torsional energy is trapped and then released.

The negative effects of mud motor back drive are severe bit-induced stick-slip which causes accelerated shoulder wear on the bit. Additionally, severe torsional cycling of the BHA causes accelerated power-section elastomer degradation (Sugiura & Jones 2021; Sugiura et al. 2022). This results in a reduction of motor output performance. The combination of these dynamic cyclic events results in a BHA trip and costly non-productive time.

Mud motor back drive is more damaging in vertical and low

angle wells due to the lack of string contact with the wellbore (the string essentially acts like a coiled spring, storing torsional energy then releasing). In horizontal wells, mud motor back drive is not as severe because of string friction against wellbore. Friction controls the extent of torsional energy build up and release.

Fig. 9 shows an example of severe mud motor back drive on a motor assist RSS BHA in a vertical 12 ¼" hole. The sensor placements are shown in the BHA diagram. The data shows that the gyro RPM spread on the mud motor bit box (in the third track from the left) and bit (in the fifth track from the left), ranging from 0RPM to 330RPM (this represents the stick-slip at the bit and BHA below the motor. The mud motor top sub gyro RPM (in the second track from the left) spreads from negative 130RPM to positive 330RPM, which indicates the mud motor back drive (negative RPM) that is traveling up the drill string.

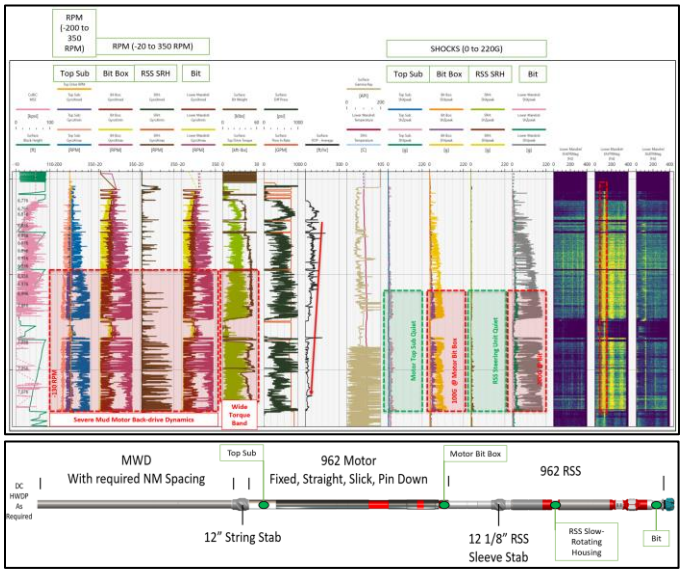

Fig. 9— Severe MMBD dynamics and HFTO combined (excerpted from SPE-212467-MS).

The associated shocks are 200G tangential (approximately 26,291 rad/s2) at the bit (in the fourth track from the right), 100G tangential (approximately 13,146 rad/s2) at the motor bit box (in the sixth track from the right), and 20G (approximately 2,629 rad/s2) at the motor top sub (in the seventh track from the right). In this example, HFTO is present below the motor and can be indirectly measured from the elevated tangential accelerations (Sugiura & Jones 2019). Of interest is the fact that the shocks in the RSS slow rotating housing are silent. This is because the RSS design utilizes a slow rotating housing mounted on mud lubricated bearings, essentially decoupling the slow rotating housing from the drive mandrel dynamics.

A good surface indicator of mud motor back drive is wide band torque. In this example, the surface torque band (green curve in the sixth track from the left) correlates good with gyro RPM spread. This is typical for a vertical or low angle example, especially when no surface torque control system is used as that can mask the response. ROP diminishes with time as the stick-slip eats away at the bit shoulder cutters reducing the effectiveness of cutting the rock (Sugiura et al. 2022).

A sample of raw gyro RPM (while rotary drilling) from drill bit and mud motor top sub is shown in **Fig. 10**. The data shows the drill bit coming to a complete stop (0 RPM) and the motor top sub reacting with negative 70 RPM being driven up the drill string. As the torsional energy from mud motor reactive torque and rig surface driven torque come together downhole (i.e. drill string torsional neutral point), the torsional energy is released causing an RPM acceleration (up to X RPM at bit and X RPM at drill string), then deceleration as the bit comes to a stop and the cycle repeats.

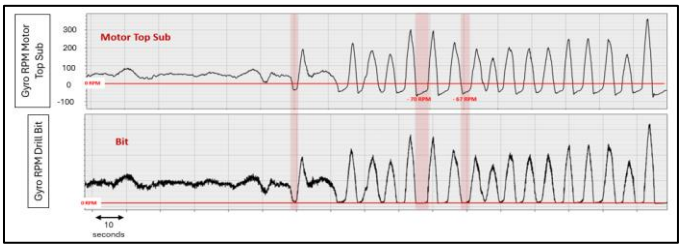

Fig. 10— Sample of Raw gyro RPM response at drill bit and mud motor top sub – MMBD dynamics

MMBD dynamics are commonplace in motor-driven RSS and conventional steerable motor assemblies. The art is to understand if these dynamics are reducing run length due to bit dull/damage, motor transmission damage and power section damage.

Removal of Mud Motor from RSS BHA

For vertical and low-angle wells, if suitable drill-pipe size and adequate top drive RPM is available, removal of the mud motor from the RSS BHA is a cost-effective way to eliminate mud motor back drive and HFTO from the BHA as shown **Fig. 11**.

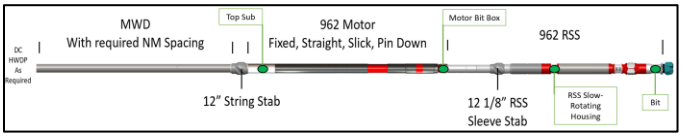

Fig. 11— RSS BHA without a mud motor

Fig. 12 shows an example of RSS dynamics in a 12 ¼" vertical hole with no mud motor. It can clearly be seen that the chaotic back-drive dynamics have disappeared, and drilling is much smoother. The gyro RPM spread at the bit (the third track from the left) is minimal, and the surface torque band (the fourth track from the left) is much healthier. The ROP remains constant throughout the run, and the bit shocks are minimal.

In this example, the removal of the mud motor led to smoother drilling and ultimately preserved the drill bit for better performance and a longer run. Removal of the mud motor can often change RSS economics in intermediate well sections and lead to a more efficient way of drilling the section versus a conventional steerable motor BHA.

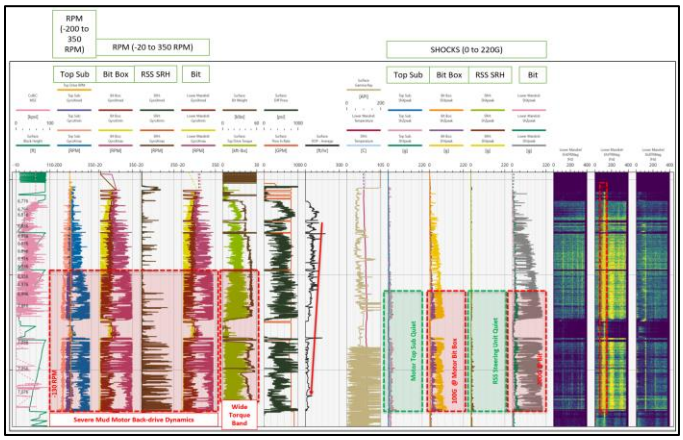

Fig. 12— Severe MMBD dynamics and HFTO combined (excerpted from SPE-212467-MS).

A sample of raw gyro RPM (while rotary drilling) from drill bit and mud motor top sub is shown in **Fig. 13**. The data shows the drill bit coming to a complete stop (0 RPM) and the motor top sub reacting with negative 70 RPM being driven up the drill string. As the torsional energy from mud motor reactive torque and rig surface driven torque come together downhole (i.e. drill string torsional neutral point), the torsional energy is released causing an RPM acceleration (up to X RPM at bit and X RPM at drill string), then deceleration as the bit comes to a stop and the cycle repeats.

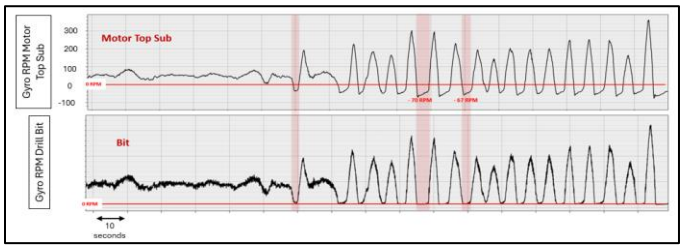

Fig. 13— Sample of Raw gyro RPM response at drill bit and mud motor top sub – MMBD dynamics
NEED BIT GYRO RPM SCALE

MMBD dynamics are commonplace in motor-driven RSS and conventional steerable motor assemblies. The art is to understand if these dynamics are reducing run length due to bit dull/damage, motor transmission damage and power section damage.

Removal of Mud Motor from RSS BHA

For vertical and low-angle wells, if suitable drill pipe size and adequate top drive RPM is available, removal of the mud motor from the RSS BHA is a cost-effective way to eliminate mud motor back drive and HFTO from the BHA.

Fig. 14 shows an example of RSS dynamics in a 12 ¼" vertical hole with no mud motor. It can clearly be seen that the chaotic back-drive dynamics have disappeared, and drilling is much smoother. The gyro RPM spread at the bit (the third track from the left) is minimal, and the surface torque band (the fourth track from the left) is much healthier. The ROP remains constant throughout the run, and the bit shocks are minimal.

In this example, the removal of the mud motor led to smoother drilling and ultimately preserved the drill bit for better performance and a longer run. Removal of the mud motor can often change RSS economics in intermediate well sections and lead to a more efficient way of drilling the section versus a conventional steerable motor BHA.

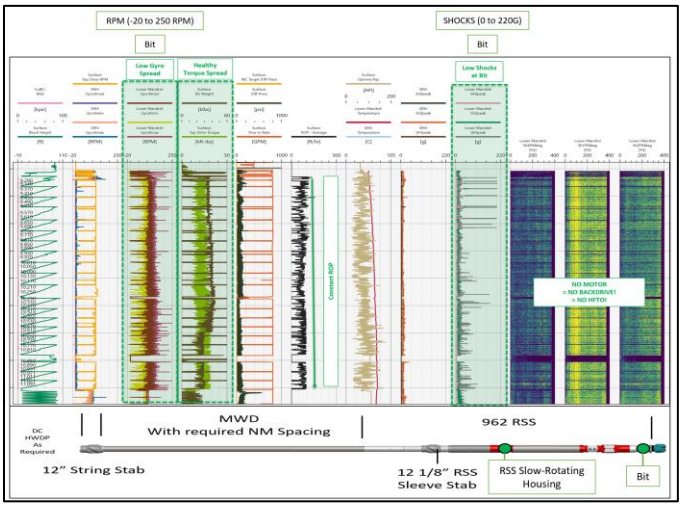

Fig. 14— Drilling dynamics with no motor in RSS BHA (excerpted from SPE-212467-MS).

Pressure-Pulse-Driven Dynamics & Power Section Degradation

MWD mud pulse dynamics is a known phenomenon that is present in all mud motor/MWD mud pulse BHAs. The MWD pressure pulse has the effect of reducing the motor output speed (bit speed) when MWD is on a pulse. Several variables dictate the magnitude of motor output "pull down while on a pulse".

Fig. 15 shows an example of mud pulse telemetry dynamics while sliding and rotating.

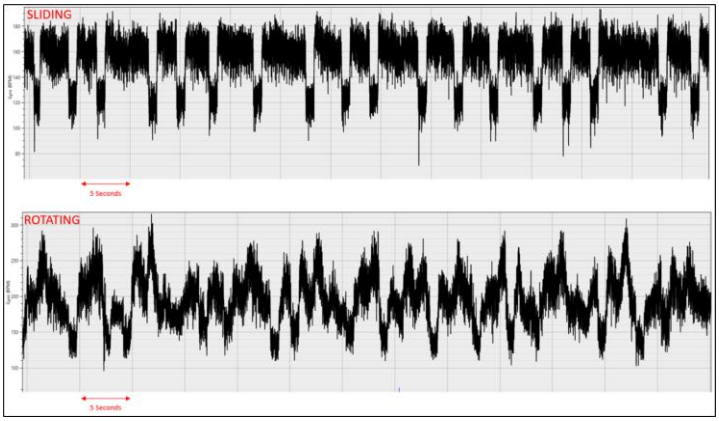

Fig. 15— Mud pulse telemetry dynamics while sliding and rotating.

Motor power section strength is a major contributor to the magnitude of bit dynamics generated from mud pulse telemetry. Degradation of the power section over time results in the MWD

pulse pulling the bit RPM to zero resulting in bit micro-stalling and eventually a full motor stall. In fact, most of the data analyzed shows that MWD mud pulse is the dominant factor that drives MMBD magnitude and mud motor stalls.

Fig. 16 shows an example of a drill bit RPM pull-down when MWD is on a pulse. The MWD pulses can clearly be seen in the bit RPM data. The bit RPM pull down on a strong power section does not have a significant effect on overall drilling performance, however as the power section degrades over time, the bit RPM pull down initiates mud motor micro stalls and eventually a full motor stall.

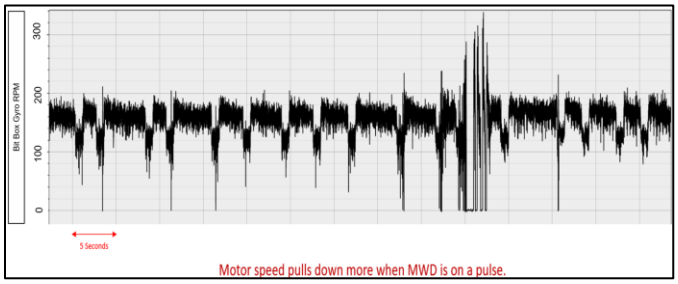

Fig. 16—The effects of an MWD mud pulse telemetry on the mud-motor output speed (excerpted from SPE-223797-MS).

Friction Reduction Tools (FRT) also generate a pulse in the drillstring (i.e. to stroke a shock tool to reduce friction between BHA and wellbore). The pulses generated by these devices are typically of a lower pulse magnitude than MWD pulses, and the placement of the FRT is a further up the drillstring away from the mud motor (2,500ft. is a common placement).

Evaluation of the pressure response above a mud motor in combination with motor output RPM shows that most FRTs do not influence pressure pulse driven dynamics. **Fig. 17** shows the pressure pulse signature from the top of a mud motor and bit rotation speed.

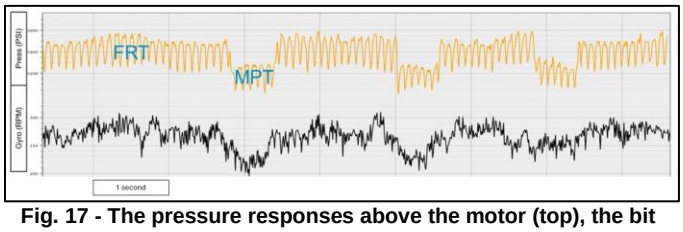

Fig. 17 - The pressure responses above the motor (top), the bit rotation speed (bottom).

The pressure signature clearly shows the pulses from the FRT at 300 PSI and 10 Hz. There is no significant correlation between FRT pulse and bit RPM. When MWD is on a pulse, the pressure drops and the associated drop in bit RPM can be seen.

Dynamics Induced from Interbedded Rock with Hard Carbonate Stringers

High-frequency sensors placed at the drill bit can identify bit dysfunction that is not seen from MWD and sensors that are placed above the mud motor. It is becoming common while drilling shale wells to encounter harder carbonate rock that with cause drill bit excitation.

Certain types of severe drill bit excitations do not necessarily cause damage to the drill bit, but they will influence mud motor transmission life. The transmission coupling on the lower end of a mud motor is typically the weakest link in the motor drivetrain, especially when subjected to combined dynamics (i.e. stick-slip, torsional oscillations, HFTO and multi-axis high magnitude shock). **Fig. 18** shows an example of severe drill bit shocks.

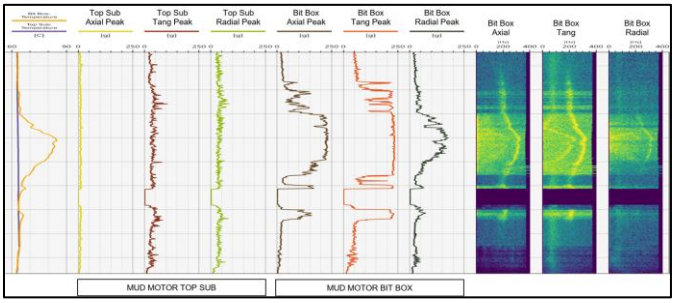

Fig. 18 - High-magnitude multi-axes shocks and bit temperature rise (excerpted from SPE-223797-MS).

3-axis shock magnitude at the bit is at severe levels (all 3-axis 200+ G) when a harder carbonate stringer is encountered. The frequencies across all three axes are very high at 300+ Hz. When the bit shock magnitude is high, a corresponding rise in bit temperature is seen. However, the key point of interest here is that the sensor placed on the top sub of the motor does not reflect any of these high-magnitude bit shocks. This is a clear demonstration that at-bit measurements are valuable when evaluating drilling performance and drill bit/motor wear/tear and failure. Without this information, post run forensics can only be speculative.

Figures 3-axis shock magnitude at the bit is at severe levels (all 3-axis 200+ G) when a harder carbonate stringer is encountered. The frequencies across all three axes are very high at 300+ Hz. When the bit shock magnitude is high, a corresponding rise in bit temperature is seen. However, the key point of interest here is that the sensor placed on the top sub of the motor does not reflect any of these high-magnitude bit shocks. This is a clear demonstration that at-bit measurements are valuable when evaluating drilling performance and drill bit/motor wear/tear and failure. Without this information, post run forensics can only be speculative.

Transitional Operations with Steerable Motors

Transitional operations with steerable motors (external bent housing) are perhaps the most common topic discussed at the present time. Typically, rotate-to-rotate and rotate-to-slide transitional operations are easier to deal with than slide-to-rotate transitions. This is because transitioning from slide drilling (gauge hole) to rotary drilling (over-gauge hole) induces higher dynamics that stresses drilling equipment. Rotate-to-slide (over-gauge to gauge hole) and rotate-to-rotate (remain in over-gauge patterned hole) do not produce the same

stress on drilling equipment, and standard drilling techniques are normally adequate.

With high bend angle steerable motors that produce high DLS yields, the technique of finishing a slide and transitioning to rotary drilling is very important for bit and mud motor preservation (especially in harder rock). Various techniques are used between different directional drilling providers depending on their experience. High-frequency downhole embedded sensors can provide a clear picture of the dynamics generated during these transitional operations and allow for transitional techniques to be experimented with and measured.

Fig. 19 shows raw gyro RPM data at the motor bit box (bottom) and motor top sub (top) during a slide-to-rotate transition. The sequence of surface operations and downhole dynamics are explained in **Table 1**.

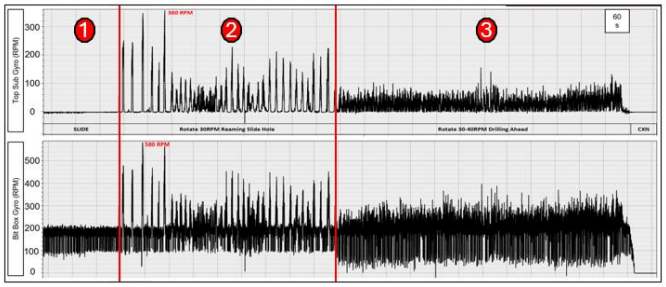

Fig. 19 - Severe torsional dynamics during a slide-to-rotate transition.

Section	Operation	Dynamics Bit Box	Dynamics Top Sub
1	On-bottom slide drilling.	Bit RPM stable. MWD mud pulse dynamics showing bit RPM reduction.	Top sub stable with surface rocking visible.
2	Pick-up through slide and start surface rotation reaming down through slid hole.	No drill bit RPM dynamics while picking up through slide with no surface rotation (gauge hole). When surface rotation started, the bit torsional oscillation peaked at 500RPM due to motor bend and bit patterning and enlarging the borehole.	No top sub dynamics while picking up through slide with no surface rotation (gauge hole). When surface rotation started, full-stall string stick-slip peaked at 360RPM due to motor bend and bit patterning and enlarging borehole.
3	On-bottom rotary drilling.	Normal drill bit torsional dynamics once BHA/bit is patterned into fresh rotary borehole. MWD mud pulse dynamics showing bit RPM reduction.	Normal string torsional dynamics once BHA/bit is patterned into fresh rotary borehole.

Table 1 – Sequence of operations reference for Figure 19.

The technique used during the slide-to-rotate transition in this example causes significant torsional dynamics that stress downhole mud motors and can damage drill bits. Exposing downhole equipment to these torsional dynamics during every slide-to-rotate operation throughout a well can be costly to the operation.

Many variables need to be considered during slide-to-rotate operations such as motor bend angle, bit-to-bend, stabilization, rock strength, mud type, etc. The optimal method to evaluate downhole dynamics during transitional operations is to measure drilling dynamics and adjust the drilling program/standard operating procedures accordingly for the area being drilled.

Combined and Switching Dynamics

As a final thought, it is worth understanding that downhole dynamics may not remain in a constant state, and there can be dynamics riding dynamics and dynamics switching.

Fig. 20 shows an example of low frequency torsional oscillation with HFTO riding. The HFTO magnitude increases (Y-axis) when the torsional oscillation RPM increases.

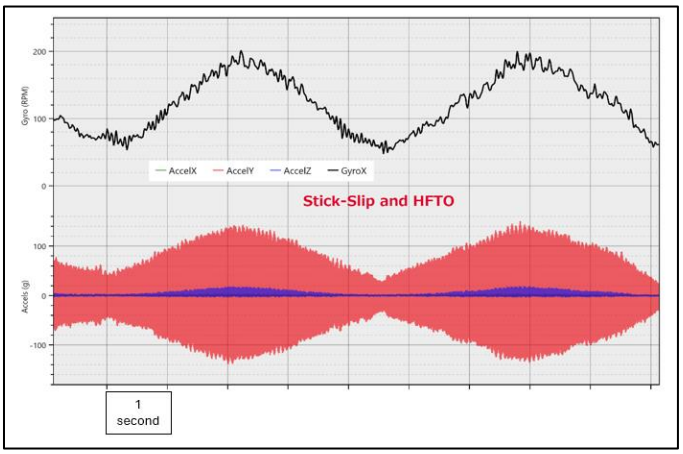

Fig. 20 – Example of low frequency torsional oscillation with HFTO riding.

Fig. 21 shows an example of dynamics switching from HFTO to MMBD. In this example the accelerometers are sampling at 800Hz and the Gyro at 100Hz. HFTO can be seen on the Y-axis accelerometer, however the gyro looks stable. This is deceiving since the gyro is sampling at 100Hz. As the frequency changes and lower frequency MMBD becomes dominant, the stick-slip can be seen on the gyro with HFTO riding the slip cycle.

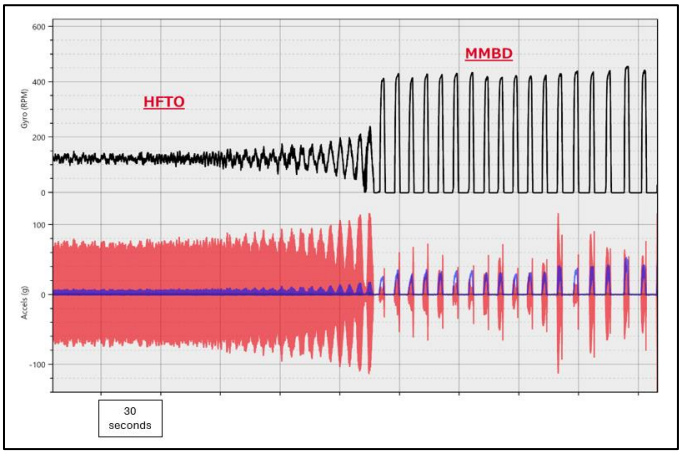

Fig. 21 – Example of dynamics switching from HFTO to MMBD.

Conclusions

High-frequency embedded drilling dynamics data is helping Permian drillers reduce costs by:

1. Identifying damaging dynamics (that cannot be seen on standard MWD S&V data)
2. Identifying damaging drilling parameters, procedures and techniques.

3. Recommending and implementing downhole tools to improve dynamics. Validating through downhole measurements.
4. Recommending and implementing parameters, procedures and techniques to improve dynamics. Validating through downhole measurements.

A host of different dynamics have been discussed in this paper, covering RSS and conventional steerable motor BHAs, as well as rig operational techniques. Many of these dynamics are commonplace in a lot of data that is analyzed in the Permian Basin today. However, every well, rig (automated, manual or remote) and set of equipment used can result in different dynamics. Spot checking dynamics with embedded sensors is a good method to understand damaging dynamics that are causing trips (frequent or sporadic).

Applying the corrective actions, measuring to validate and implementing standard operating procedures will lead to consistent and repeatable well construction that will result in reduced operating costs.

Acknowledgments

The authors would like to thank Sanvean Technologies, LLC for their willingness to publish the digital data and for permitting the publication of this work.

Nomenclature

BHA = Bottomhole Assembly
DLS = Dogleg Severity
FRT = Friction Reduction Tool
HFTO = High-Frequency Torsional Oscillation
MWD = Measurement While Drilling
PF = Plastic Viscosity
ROP = Rate of Penetration
RPM = Revolutions per Minute
RSS = Rotary Steerable System
S&V = Shock and Vibration

References

Adam, Derek "Reducing Stick-Slip by Avoiding Auto-Driller Control Dysfunction." Paper presented at the IADC/SPE Drilling Conference and Exhibition, Fort Worth, Texas, USA, March 2018. doi: https://doi.org/10.2118/189653-MS.

Brett, J. F. (1992, September 1). The Genesis of Bit-Induced Torsional Drillstring Vibrations. Society of Petroleum Engineers. doi:10.2118/21943-PA.

Crew, H. (2008). *The Principles of Mechanics*. BiblioBazaar, LLC.

Chen, S., Wisinger, J., Dunbar, B., & Propes, C. (2020, February 25). Identification and Mitigation of Friction- and Cutting Action-Induced Stick-Slip Vibrations with PDC Bits. Society of Petroleum Engineers. doi:10.2118/199639-MS.

Close, D.A., Owens, S.C., and MacPherson, J.D. 1988. Measurement of BHA Vibration Using MWD. Presented at the SPE/IADC Drilling Conference, Dallas, Texas, USA, 28 February–2 March. SPE-17273-MS. http://dx.doi.org/10.20118/17273-MS.

Dupriest, F., Noynaert, S., & Cunningham, T. (2020, March). *Maximizing Drilling Performance Through the Delaware Basin Brushy Canyon and Interbedded Formations.* Paper presented at the IADC/SPE International Drilling Conference and Exhibition, Galveston Texas USA, SPE-199599-MS. doi: https://doi.org/10.2118/199599-MS.

Fonseca, I. S., Isbell, M., and Groover, A. "Applying a Downhole Drilling Mechanics Tool to Improve Operational Procedures and Rig Operating Systems in Horizontal Wells." Paper presented at the SPE/IADC International Drilling Conference and Exhibition, Stavanger, Norway, March 2023. doi: https://doi.org/10.2118/212520-MS

Halsey, G. W., Kyllingstad, A., Aarrestad, T. V., & Lysne, D. (1986, January 1). Drillstring Torsional Vibrations: Comparison Between Theory and Experiment on a Full-Scale Research Drilling Rig. Society of Petroleum Engineers. doi:10.2118/15564-MS.

Isbell, M., Neal, J., Copeland, H., Foster, N., and Patrick, S. "Maximizing the Value of Downhole Drilling Data: A Novel Approach to Digital Drilling Data Management and Analytics." Paper presented at the IADC/SPE International Drilling Conference and Exhibition, Galveston, Texas, USA, March 2022. doi: https://doi.org/10.2118/208710-MS.

Jain, J. R., Oueslati, H., Hohl, A. et al. 2014. High-Frequency Torsional Dynamics of Drilling Systems: An Analysis of the Bit-System Interaction. Presented at the IADC/SPE Drilling Conference and Exhibition, Fort Worth, Texas, 4–6 March. SPE-167968-MS. https://doi.org/10.2118/167968-MS.

Jones, S., Sugiura, J., Rose, K., and Schnuriger, M. "Drilling Dynamics Data Recorders Now Cost-Effective for Every Operator - Compact Embedded Sensors in Bit and BHA Capture Small Data to Make the Right Decisions Fast." Paper presented at the SPE/IADC Drilling Conference and Exhibition, The Hague, The Netherlands, March 2017. doi: https://doi.org/10.2118/184738-MS.

Jones, S., & Sugiura, J. "Real-Time Drilling Advisory Roadmap System Delivers Superior Performance When Used in Conjunction with Downhole Embedded Drilling Dynamics Sensors." Paper presented at the IADC/SPE International Drilling Conference and Exhibition, Galveston, Texas, USA, March 2020. doi: https://doi.org/10.2118/199560-MS.

Jones, S., Sugiura, J., and Johnson, D.W. "Rotary Steerable Drilling Dynamics and Associated BHA Changes to Improve Overall BHA Performance and Reliability." Paper presented at the SPE/IADC International Drilling Conference and Exhibition, Stavanger, Norway, March 2023. doi: https://doi.org/10.2118/212467-MS.

Kyllingstad, A., & Halsey, G. W. (1987, January 1). A Study of Slip-Stick Motion of the Bit. Society of Petroleum Engineers. doi:10.2118/16659-MS.

Ledgerwood, L. W., Hoffmann, O. J., Jain, J. R., El Hakam, C., Herbig, C., & Spencer, R. (2013, January 1). Downhole Vibration Measurement, Monitoring, and Modeling Reveal Stick/Slip as a Primary Cause of PDC-Bit Damage in Today. Society of Petroleum Engineers. doi:10.2118/134488-PA.

Lines, L. A., Stroud, D. R. H., and Coveney, V. A. 2013. Torsional Resonance—An Understanding Based on Field and Laboratory Tests With Latest Generation Point-the-Bit Rotary Steerable System. Presented at the SPE/IADC Drilling Conference, Amsterdam, The Netherlands, 5–7 March. SPE163428-MS. https://doi.org/10.2118/163428-MS.

Lubinski, A., & Althouse, W.S. “Helical Buckling of Tubing Sealed in Packers.” Journal of Petroleum Technology 14 (1962): 655-670.

Oueslati, H., Jain, J. R., Reckmann, H., Ledgerwood, L.W.III, Pessier, R., and Chandrasekaran, S., "New insights into drilling dynamics through high frequency vibration measurement and modeling", Paper SPE-166212 presented at SPE Annual Technical Conference

and Exhibition, New Orleans, USA, 30 September – 2 October 2013. doi: https://doi.org/10.2118/166212-MS

Pastusek, P., Sullivan, E., and Harris, T. "Development and Utilization of a Bit-Based Data-Acquisition System in Hard-Rock PDC Applications." Paper presented at the SPE/IADC Drilling Conference, Amsterdam, The Netherlands, February 2007. doi: https://doi.org/10.2118/105017-MS.

Pastusek, P., Owens, M., Barrette, D., Wilkins, V., Bolzan, A., Ryan, J., Akyabi, K., Reichle, M., and Pais, D. "Drill Rig Control Systems: Debugging, Tuning, and Long Term Needs." Paper presented at the SPE Annual Technical Conference and Exhibition, Dubai, UAE, September 2016. doi: https://doi.org/10.2118/181415-MS.

Pastusek, P., Sanderson, D., Minkevicius, A., Blakeman, Z., Bailey, J., "Drilling Interbedded and Hard Formations with PDC Bits Considering Structural Integrity Limits" Paper presented at the IADC/SPE Drilling Conference and Exhibition, Ft Worth, TX, March 2018, doi: https://doi.org/10.2118/189608-MS

Sugiura, J., & Jones, S. "A Drill Bit and a Drilling Motor With Embedded High-Frequency (1600 Hz) Drilling Dynamics Sensors Provide New Insights Into Challenging Downhole Drilling Conditions." SPE Drill & Compl 34 (2019): 223–247. doi: https://doi.org/10.2118/194138-PA.

Sugiura, J., & Jones, S. "Simulation and Measurement of High-Frequency Torsional Oscillation (HFTO)/High-Frequency Axial Oscillation (HFAO) and Downhole HFTO Mitigation: Knowledge Gains Continue Using Embedded High-Frequency Drilling Dynamics Sensors." SPE Drill & Compl 35 (2020): 553–575. doi: https://doi.org/10.2118/199658-PA.

Sugiura, J., & Jones, S. "Measurement of Mud Motor Back-Drive Dynamics, Associated Risks, and Benefits of Real-Time Detection and Mitigation Measures." SPE Drill & Compl (2021;): doi: https://doi.org/10.2118/204032-PA.

Sugiura, J., Jones, S., and Pastusek P. "A Systematic Photo Documentation of Drill Bit Forensics Applied to Motor Back-Drive Dynamics Case Caused by Auto-Driller Dysfunction and Formation Effect." Paper presented at the SPE Annual Technical Conference and Exhibition, Houston, Texas, USA, October 2022. doi: https://doi.org/10.2118/210466-MS.

Tuplin, W.A. (1966). *Torsional Vibrations*, Pitman, London.

Watson, W., Dupriest, F., Witt-Doerring, Y., Pastusek, P., Sugiura, J., Procter, R., Daechsel, D., Abbas, R., and Shackleton, D. "IADC Code Upgrade: Bit and BHA Forensics Using Rig-Based Photographic Documentation Practices." Paper presented at the IADC/SPE International Drilling Conference and Exhibition, Galveston, Texas, USA, March 2022. doi: https://doi.org/10.2118/208707-MS.

Watson, W., Dupriest, F., Witt-Doerring, Y., Sugiura, J., Pastusek, P., Daechsel, D., Abbas, R., and Shackleton, D. "IADC Code Upgrade: Data Collection and Workflow Required to Conduct Bit Forensics and Create Effective Changes in Practices or Design." Paper presented at the IADC/SPE International Drilling Conference and Exhibition, Galveston, Texas, USA, March 2022. doi: https://doi.org/10.2118/208712-MS.

Watson, W., Witt-Doerring, Y., Sugiura, J., Pastusek, P., Daechsel, D., Vallet, L., Amish, M., and Oluyemi, G. "IADC Code Upgrade: Interpretation of Surface and Downhole Data to Support Drilling Forensics." Paper presented at the SPE Annual Technical Conference and Exhibition, Houston, Texas, USA, October 2022. doi: https://doi.org/10.2118/210243-MS.

Wilson, W.K. (1956). *Practical Solution of Torsional Vibration Problems*, Vol. I Chapman & Hall.

Zannoni, S. A., Cheatham, C. A., Chen, C.-K. D., & Golla, C. A. (1993, January 1). Development and Field Testing of a New Downhole MWD Drillstring Dynamics Sensor. Society of Petroleum Engineers. doi:10.2118/26341-MS.